

# ANALYSIS OF THE SPATIOTEMPORAL EVOLUTION CHARACTERISTICS AND SPATIAL HETEROGENEITY DRIVING MECHANISMS OF REGIONAL PM2.5 BASED ON MGWR: A CASE STUDY IN CENTRAL CHINA

LU, B. – ZHANG, M. C.\* – WANG, Y. W. – WANG, K. D. – LI, X. F. – WANG, H.

*School of Computer Science and Technology, Zhengzhou University of Light Industry, 450000  
Zhengzhou, China*

*\*Corresponding author  
e-mail: yanzhi\_zmc@163.com*

(Received 21<sup>st</sup> May 2024; accepted 18<sup>th</sup> Oct 2024)

**Abstract.** The presence of particulate matter smaller than 2.5  $\mu\text{m}$  (PM2.5), one of the major air pollutants, exerts a significant detrimental impact on human health, the natural environment, and the sustainable development of society and the economy. Consequently, it has become imperative to conduct comprehensive research on its spatiotemporal evolution characteristics as well as the underlying driving factors. In order to comprehensively investigate the spatiotemporal evolution of PM2.5 and elucidate the underlying driving mechanisms considering spatial heterogeneity, this study utilized 22 years of remote sensing data on PM2.5 in central China to establish a standard deviation ellipse model and conduct spatial autocorrelation analysis. Additionally, it integrated normalized difference vegetation index (NDVI), gross domestic product (GDP), and other factors to construct a multi-scale geographical weighted regression model (MGWR). The findings are as follows: (1) Over the past 22 years, the annual average concentration of PM2.5 in central China has generally declined, but most of Henan Province and central Hubei Province remain key areas of PM2.5 pollution. (2) Spatially, there is evident aggregation of PM2.5 concentration, with hot spots predominantly concentrated in Henan Province and cold spots mainly found in Hunan Province. (3) The precision of spatial data can have a certain degree of impact on the results of driving models. Compared to GWR, MGWR can more effectively capture the spatial heterogeneity of influencing factors at different scales. (4) Varying degrees of spatial heterogeneity are indicated by the results that are obtained from the MGWR in different factors impacting PM2.5 concentration in Central China. Therefore, it is crucial to consider spatial heterogeneity when modeling and analyzing data with spatial attributes.

**Keywords:** *aerosol, environmental sustainability, spatial heterogeneity, air quality, multi-scale*

## Introduction

The advancement of the economy and the enhancement of people's living standards have led to an increasing public concern for ecological safety. Air pollution poses a significant challenge that humanity must confront during the process of industrialization. The atmospheric pollutant PM2.5 is widely recognized as a significant contributor to environmental degradation and poses serious threats to human health (Chen et al., 2020; Yang et al., 2022b). The term "PM2.5" refers to airborne particles with an aerodynamic equivalent diameter of 2.5 microns or less in ambient air. These particles have the ability to remain suspended in the air for extended periods, and as the concentration of these particles increases, so does the severity of air pollution. Therefore, it is imperative to conduct in-depth research on the spatiotemporal evolution characteristics and associated driving factors of PM2.5, considering both public health implications and the sustainable development of society and the environment.

From the perspective of study area and scale, numerous scholars both domestically and internationally have conducted analyses on the spatiotemporal distribution patterns of PM2.5 as well as its associated driving factors across various spatial scales. Consequently, a comprehensive multi-scale research framework has been established encompassing countries (Xie et al., 2016; Lin et al., 2014; He et al., 2021), river basins (Jiang et al., 2021; He et al., 2019; Zhao et al., 2022), urban agglomerations (Shen et al., 2019; Huang et al., 2021; Liu et al., 2020), provinces (Gu et al., 2010; Zhang et al., 2020; Huang et al., 2020), and prefecture-level cities (Yang et al., 2022a; Fang et al., 2016; Wang et al., 2023). However, the majority of these studies primarily focus on the relatively developed regions within China. Central China, with its large population and status as one of China's important economic regions, has experienced higher levels of PM2.5 pollution compared to other regions. Given the prominent position that the state has placed on the construction of ecological civilization, addressing atmospheric environmental pollution is crucial for both public health and sustainable economic development.

From the perspective of research methods and directions, in terms of analyzing the spatiotemporal distribution characteristics of PM2.5, scholars primarily investigate its change patterns over time and space, as well as its spatial correlations through various methodologies such as yearly and monthly data analysis, changes in spatial center of gravity, spatial hot spot analysis, among others (Yan et al., 2022; Zhu et al., 2022; Fan et al., 2017; Yuan et al., 2021; Wang et al., 2022). Among these mechanisms, the modification in gravity's spatial center can be effectively determined utilizing the standard deviation elliptic (SDE) model (Shi et al., 2018), which not only calculates the spatial center of the concentration but also accurately reflects directional distribution of PM2.5 across space. Regarding the analysis of PM2.5 driving mechanisms, currently employed modeling methods can be categorized into traditional techniques like ordinary least squares analysis (Fang et al., 2020), rank correlation analysis (Chang et al., 2017), grey correlation analysis (Ouyang et al., 2018), etc., along with approaches from a spatial perspective such as residual analysis (Tu et al., 2021), spatial Durbin model (Chen et al., 2019), and geographical weighted regression (GWR) model (Luo et al., 2017). The PM2.5 concentration, being a data with spatial properties, exhibits distinct spatial heterogeneity in its relationship with various influencing factors (Wang et al., 2020). Sources of PM2.5 pollution encompass both natural and anthropogenic origins. Natural sources include volcanic eruptions, forest fires, hurricanes, tsunamis, weathering of soil and rocks, and biological decay, which contribute to the introduction of fine particles into the atmosphere as part of PM2.5. Anthropogenic sources primarily stem from human activities and industrial production processes and serve as the main contributors to PM2.5 levels. Simultaneously, both the natural environment and human intervention can mitigate PM2.5 pollution through various means. To effectively curb PM2.5 pollution requires understanding the relationship between PM2.5 concentration and its associated influencing factors. At the same time, the natural and socio-economic influencing factors of PM2.5 concentration are also data with spatial properties. Hence, it is crucial to unveil the effect of spatial heterogeneity in driving factors when analyzing the mechanism behind PM2.5. The multi-scale geographical weighted regression (MGWR) model is an enhanced version of GWR that incorporates the spatial heterogeneity of drivers and their functions (Fotheringham et al., 2017), offering a novel approach to modeling spatial data drivers.

In summary, this study focuses on Central China as the research area and utilizes 22 years of PM2.5 remote sensing data and high-resolution raster data of impact factors to analyze the spatiotemporal distribution characteristics of PM2.5 using SDE.

Additionally, it investigates the spatial aggregation patterns of PM<sub>2.5</sub> through spatial autocorrelation and hot spot analysis. Furthermore, the MGWR is employed to uncover the influence of driving factors on the distribution and spatial heterogeneity of PM<sub>2.5</sub>, thereby providing valuable insights for analyzing PM<sub>2.5</sub> pollution and formulating atmospheric environment policies.

## Materials and methods

### Study area

Central China encompasses Henan, Hubei, and Hunan provinces. Spanning over 560,000 km<sup>2</sup>, it accounts for approximately 5.9% of the country's total land area. With a robust industrial foundation and advanced agricultural production capabilities, Central China serves as a vital energy and raw materials base while also functioning as an extensive transportation hub. The region is abundant in human resources and scientific educational facilities that significantly influence China's overall economic development. With the implementation of the Central China Rise strategy, its economy has experienced rapid growth, establishing itself as a pivotal region for industrial advancement in the country. However, amidst this progress lies a pressing concern regarding air quality in Central China; thus, necessitating further strengthening of environmental governance. The study area is shown in *Figure 1*.

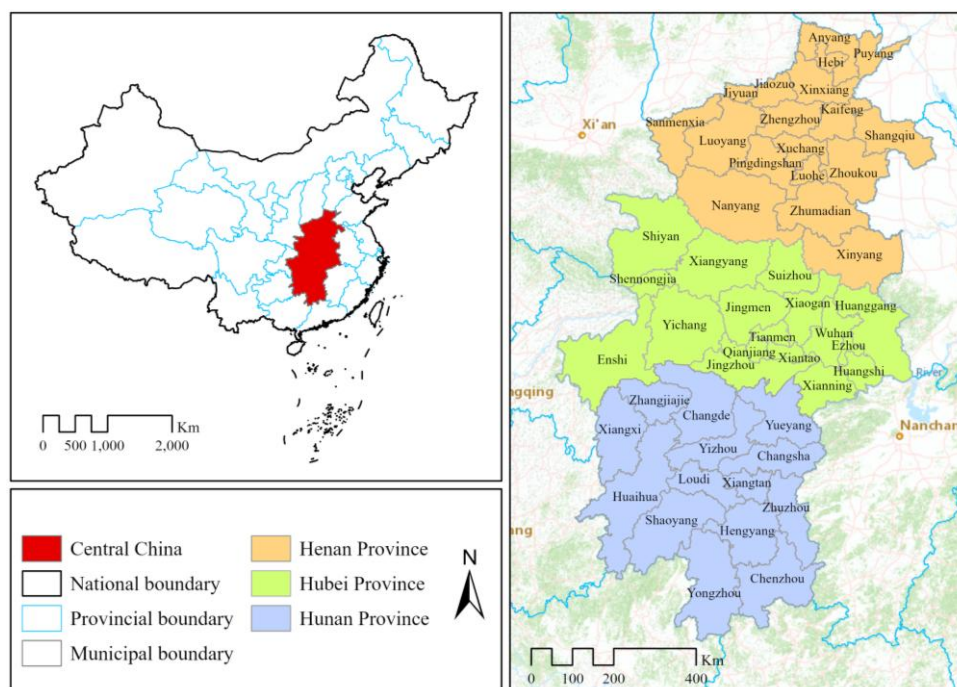


**Figure 1.** Geographical location and administrative divisions of Central China

### Data source

#### PM<sub>2.5</sub> data

The PM<sub>2.5</sub> raster data acquired through remote sensing inversion are sourced from the Atmospheric Composition Analysis Group at the Washington University in St.

Louis (V5.GL.04). The data has a spatial resolution of  $1 \text{ km} \times 1 \text{ km}$ , enabling a more accurate representation of the actual spatial distribution of PM2.5.

#### Other data

In order to analyze the driving mechanism of PM2.5 spatial concentration, this study incorporated two types of impact factor data: natural and socio-economic data. The natural data encompass air temperature, vegetation index, average wind speed, relative humidity, elevation, and precipitation. Socio-economic data encompass night lighting, CO2 emissions, electricity consumption, population density, GDP, and proportion of arable land. The data sources and their corresponding descriptions are presented in Table 1.

**Table 1.** Influencing factors and description of PM2.5 concentration

Type	Factor	Description and data source
Natural factors	X1: air temperature	Average annual temperature at $1 \text{ km} \times 1 \text{ km}$ resolution/ $^{\circ}\text{C}$ ( <a href="https://cstr.cn/18406.11.Meteoro.tpd.c.270961">https://cstr.cn/18406.11.Meteoro.tpd.c.270961</a> )
	X2: vegetation index	Vegetation index at $1 \text{ km} \times 1 \text{ km}$ resolution/NDVI ( <a href="https://modis.gsfc.nasa.gov/data/dataproduct/mod13.php">https://modis.gsfc.nasa.gov/data/dataproduct/mod13.php</a> )
	X3: wind speed	Average annual wind speed at $1 \text{ km} \times 1 \text{ km}$ resolution/(m/s) ( <a href="http://www.geodata.cn/data/datadetails.html?dataguid=3796451&amp;docid=5735">http://www.geodata.cn/data/datadetails.html?dataguid=3796451&amp;docid=5735</a> )
	X4: relative humidity	Relative humidity at $1 \text{ km} \times 1 \text{ km}$ resolution/(kg/kg) ( <a href="http://www.geodata.cn/data/datadetails.html?dataguid=126928059243667&amp;docId=11969">http://www.geodata.cn/data/datadetails.html?dataguid=126928059243667&amp;docId=11969</a> )
	X5: elevation	Elevation at $1 \text{ km} \times 1 \text{ km}$ resolution/(m) ( <a href="https://www.gscloud.cn/">https://www.gscloud.cn/</a> )
	X6: precipitation	Precipitation at $1 \text{ km} \times 1 \text{ km}$ resolution/(mm) ( <a href="http://www.geodata.cn/data/datadetails.html?dataguid=2329433&amp;docId=7668">http://www.geodata.cn/data/datadetails.html?dataguid=2329433&amp;docId=7668</a> )
Socio-economic factors	X7: nighttime light	Nighttime light at $1 \text{ km} \times 1 \text{ km}$ resolution/(LUX) ( <a href="https://data.tpd.ac.cn/zh-hans/data/e755f1ba-9cd1-4e43-98ca-cd081b5a0b3e">https://data.tpd.ac.cn/zh-hans/data/e755f1ba-9cd1-4e43-98ca-cd081b5a0b3e</a> )
	X8: CO2 emission	CO2 emission at $1 \text{ km} \times 1 \text{ km}$ resolution/(tons/ $\text{km}^2$ ) ( <a href="https://cger.nies.go.jp/en/">https://cger.nies.go.jp/en/</a> )
	X9: electricity consumption	Electricity consumption at $1 \text{ km} \times 1 \text{ km}$ resolution/(Kwh) ( <a href="https://www.nature.com/articles/s41597-022-01322-5">https://www.nature.com/articles/s41597-022-01322-5</a> )
	X10: population density	Population density at $1 \text{ km} \times 1 \text{ km}$ resolution/(persons/ $\text{km}^2$ ) ( <a href="https://landscan.ornl.gov/">https://landscan.ornl.gov/</a> )
	X11: GDP	GDP emission at $1 \text{ km} \times 1 \text{ km}$ resolution/(ten thousand yuan/ $\text{km}^2$ )( <a href="https://www.resdc.cn/DOI/DOI.aspx?DOIID=33">https://www.resdc.cn/DOI/DOI.aspx?DOIID=33</a> )
	X12: arable land area share	Arable land area share at $30\text{m} \times 30\text{m}$ resolution/(%) ( <a href="https://essd.copernicus.org/articles/13/3907/2021/">https://essd.copernicus.org/articles/13/3907/2021/</a> )

Considering the potential presence of multicollinearity among the selected driver variables in this study, we employed VIF (variance inflation factor) to examine all the

aforementioned explanatory variables. This was done to mitigate any bias in the estimated results caused by intercorrelations between indicators. A higher VIF value indicates a greater degree of multicollinearity, and it is generally accepted that a variable is highly collinear if its VIF value exceeds 10. The reciprocal of VIF represents tolerance, with values closer to zero indicating stronger multicollinearity. The VIF is calculated as follows:

$$VIF = \frac{1}{1 - R_i^2} \sum_{i=1}^n X_i \quad (\text{Eq.1})$$

The multiple correlation coefficient represents the relationship between the *i*th independent variable and the remaining independent variables in regression analysis. The test results are presented in *Table 2*. Each index has a variance inflation factor value below 10, indicating the absence of multicollinearity issues among the selected indices.

**Table 2.** Multicollinear detection of influencing factors

Variable	X1	X2	X3	X4	X5	X6	X7	X8	X9	X10	X11	X12
VIF	5.544	1.692	1.497	3.080	2.210	6.136	1.719	3.003	1.017	2.664	1.214	2.667
Tolerance	0.180	0.591	0.668	0.325	0.453	0.163	0.582	0.333	0.983	0.375	0.823	0.374

## Research methodology

### Standard deviation ellipse analysis

The SDE model is a statistical method utilized for characterizing the distribution characteristics of spatial data. This model computes the range, direction, and shape of data points to determine the center of gravity, concentration direction, and contraction trend of spatial data.

The center of the ellipse in this study represents the centroid of the PM2.5 concentration data distribution in a two-dimensional space, while the area of the ellipse indicates the spatial extent of PM2.5 distribution. The center of the ellipse is determined by the following calculation.

$$\bar{X}_w = \frac{\sum_{i=1}^n w_i x_i}{\sum_{i=1}^n w_i} \quad (\text{Eq.2})$$

$$\bar{Y}_w = \frac{\sum_{i=1}^n w_i y_i}{\sum_{i=1}^n w_i} \quad (\text{Eq.3})$$

The weight of object *i* is represented by *w<sub>i</sub>*, and the spatial coordinate position of the research object *i* is denoted by (*x<sub>i</sub>*, *y<sub>i</sub>*).

The azimuth angle represents the predominant directional trend of the distribution of PM2.5. Changes in the azimuth angle can reflect alterations in the primary directional trend of PM2.5 distribution. The formula for computing azimuth Angle  $\theta$  is as follows:

$$\tan \theta = \frac{\left( \sum_{i=1}^n w_i^2 x_i^2 - \sum_{i=1}^n w_i^2 y_i^2 \right) + \sqrt{\left( \sum_{i=1}^n w_i^2 x_i^2 - \sum_{i=1}^n w_i^2 y_i^2 \right) + 4 \sum_{i=1}^n w_i^2 x_i y_i}}{2 \sum_{i=1}^n w_i^2 x_i y_i} \quad (\text{Eq.4})$$

The variables  $(x_i, y_i)$  in the given equation represent the spatial displacement from the central point  $(\bar{X}_w, \bar{Y}_w)$  to the coordinates of PM2.5 data within the study area.

The ellipse's major and minor axes correspond to the principal directions in the dataset. The formula for computing the major and minor semi-axes is as follows:

$$\sigma_x = \sqrt{\frac{\sum_{i=1}^n (w_i x_i \cos \theta - w_i y_i \sin \theta)^2}{\sum_{i=1}^n w_i^2}} \quad (\text{Eq.5})$$

$$\sigma_y = \sqrt{\frac{\sum_{i=1}^n (w_i x_i \sin \theta - w_i y_i \cos \theta)^2}{\sum_{i=1}^n w_i^2}} \quad (\text{Eq.6})$$

### *Spatial autocorrelation analysis*

The concept of spatial autocorrelation is employed to depict the interdependence between neighboring geographical locations as well as the temporal interdependence among different locations in terms of variables. Given that PM2.5 concentration data possesses spatial attributes, examining its presence of spatial autocorrelation characteristics facilitates a more comprehensive investigation into the spatiotemporal evolution patterns of PM2.5. Spatial autocorrelation can be categorized into global and local types, with global autocorrelation commonly utilized as a Moran index. The formula for computing the Moran index is as follows:

$$I = \frac{\sum_{i=1}^n \sum_{j=1}^n w_{ij} (X_i - \bar{X})(X_j - \bar{X})}{\left( \frac{1}{n} \sum_{i=1}^n X_i - \bar{X} \right)^2 \sum_{i=1}^n \sum_{j=1}^n w_{ij}} \quad (\text{Eq.7})$$

In this equation,  $I$  stands for the Moran index, while  $n$  represents the total figure of cells.  $X_i$  and  $X_j$  denote the PM2.5 concentrations of cells  $i$  and  $j$ , respectively.  $w_{ij}$  indicates

the spatial weight between cells  $i$  and  $j$ , where a value of 1 signifies contiguity and 0 signifies non-contiguity.  $\bar{X}$  signifies the sample average.

#### *Hot spot analysis with rendering*

The Moran Index provides a comprehensive measure of the spatial autocorrelation of PM2.5. To further investigate the spatial clustering patterns of PM2.5, this study employs hotspot analysis to examine local autocorrelation.

$$G_i^* = \frac{\sum_{j=1}^n W_{ij} x_j - \bar{X} \sum_{j=1}^n W_{ij}}{S \sqrt{\frac{n \sum_{j=1}^n W_{ij}^2 - \left( \sum_{j=1}^n W_{ij} \right)^2}{n-1}}} \quad (\text{Eq.8})$$

$$\bar{X} = \frac{\sum_{j=1}^n X_j}{n} \quad (\text{Eq.9})$$

$$S = \sqrt{\frac{\sum_{j=1}^n X_j^2}{n} - \bar{X}^2} \quad (\text{Eq.10})$$

In this circumstance, the total number of PM2.5 data cells is represented by  $n$ ;  $X_j$  is the attribute value of data cell  $j$ ;  $W_{ij}$  denotes the spatial adjacency between cell  $i$  and  $j$ ;  $S$  relates to the overall mean standard deviation of PM2.5 in the study region. A high value of  $G_i^*$  signifies a dense clustering of hot spots.

#### *Geographically weighted regression*

The GWR can partially address spatial autocorrelation and spatial non-stationarity issues that are beyond the capabilities of the OLS model. The fundamental formula is as follows:

$$Y_i = \beta_0(u_i, v_i) + \sum_{j=1}^n \beta_j(u_i, v_i) X_{ij} + \varepsilon_i \quad (\text{Eq.11})$$

where  $i$  represents a sample unit,  $(u_i, v_i)$  is the spatial coordinate of unit  $i$ ,  $Y_i$  denotes the annual average mass concentration of PM2.5 for unit  $i$  and  $X_{ij}$  corresponds to the  $j$ th explanatory variable of unit  $i$ . The constant term of unit  $i$  is denoted by  $\beta_0(u_i, v_i)$ , the regression parameter of the independent variable in the data sampling point is denoted by  $\beta_j(u_i, v_i)$ , and  $\varepsilon_i$  represents a random error component.

### *Multiscale geographically weighted regression*

The MGWR model is an extension of GWR that allows for varying neighborhood sizes around each spatial element for different explanatory variables. This flexibility enables the coefficients of certain variables to change gradually and weakly across the study area, while others can exhibit rapid changes. By matching the neighborhood scale with each explanatory variable's spatial scale, MGWR provides a novel approach to accurately analyze the correlation between spatial data.

$$Y_i = \beta_{bw0}(u_i, v_i) + \sum_{j=1}^n \beta_{bwj}(u_i, v_i) X_{ij} + \varepsilon_i \quad (\text{Eq.12})$$

The  $bw_j$  represents the bandwidth used for the regression coefficients of the  $j$ th variable. That is, *Equation 12* differs from *Equation 11* in that  $\beta_{bwj}(u_i, v_i)$  represents the regression coefficient of  $bw_j$  bandwidth for the  $j$ th variable at the  $i$  sample point. The MGWR model was calibrated using the inverse fitting algorithm proposed by Fotheringham et al. (Fotheringham et al., 2017; Yu et al., 2020).

The construction of the MGWR model in this paper was based on the development of MGWR2.2 software by the Spatial Analysis Research Center (SPARC) at Arizona State University (<https://sgsup.asu.edu/SPARC>).

## **Results**

### *Temporal variation pattern of PM2.5 concentration*

Based on PM2.5 remote sensing data, the average annual PM2.5 concentration in Central China and its various provinces and cities during the period from 2000 to 2021 was calculated. The *Figure 2* illustrates that there was an initial increase followed by a subsequent decrease in the average annual PM2.5 concentration in Central China between 2000 and 2021. Notably, the three provinces exhibited distinct levels of PM2.5 concentration, with Henan Province displaying significantly higher values compared to Hubei and Hunan provinces, thus establishing itself as the most severely affected area by PM2.5 pollution in central China. Moreover, Hubei had slightly higher average annual PM2.5 concentrations than Hunan, while both regions demonstrated a similar inverted “V”-shaped trend overall, reaching their respective peaks in 2011.

Among them, Henan Province as a whole exhibited a distinct “M” shaped trend in terms of air pollution levels. The peak concentrations were recorded in 2007 and 2013, reaching 73.35  $\mu\text{g}/\text{m}^3$  and 73.85  $\mu\text{g}/\text{m}^3$  respectively. In Hubei and Hunan provinces, the concentrations of PM2.5 reached their peak in 2011 at levels of 60.46  $\mu\text{g}/\text{m}^3$  and 55.21  $\mu\text{g}/\text{m}^3$  respectively.

From the perspective of each city in Henan Province, as depicted in *Figure 3*, the highest average annual PM2.5 concentration is exhibited by Xinxiang and Jiaozuo among the 18 cities, which can be attributed to their local industrial and energy structures. The dominance of heavy industry and energy production in these areas significantly impacts the environment. Additionally, the abundance of coal resources coupled with a reliance on thermal power generation further exacerbates PM2.5 pollution levels. Conversely, Luoyang and Jiyuan experience relatively low average



annual PM2.5 concentrations due to specific factors unique to each city's location and industrial structure. Luoyang's western position within Henan Province results in a dry and cold climate that hinders the accumulation of PM2.5 pollutants; this is also indicative of the positive environmental impact achieved through the implementation of "Luoyang ban fireworks regulations" by the Luoyang Municipal Bureau of Ecological Environment in 2005. On the other hand, Jiyuan's predominantly light industry-based industrial structure has comparatively minimal impact on its environment.

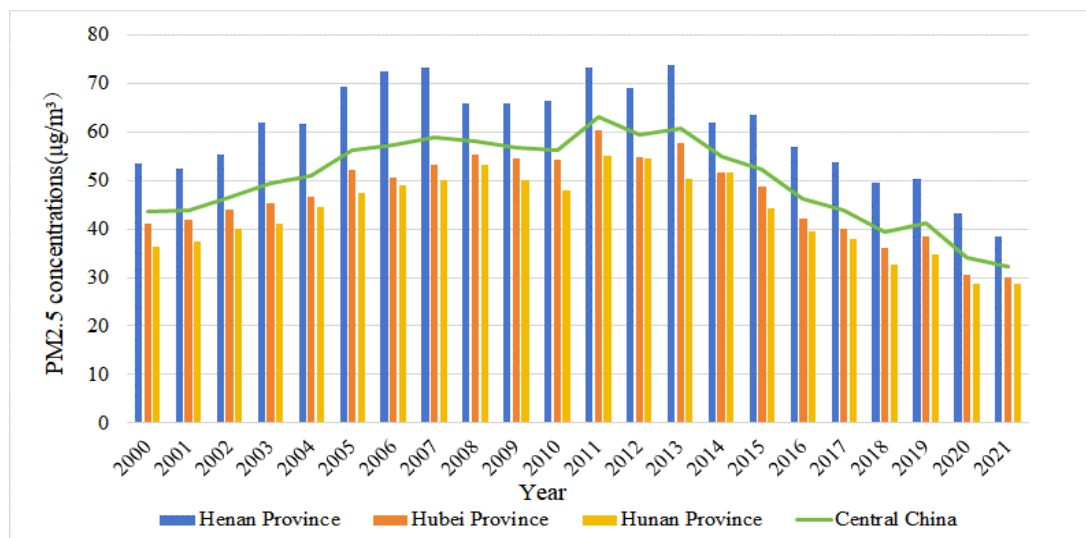


**Figure 2.** Variation trend of the average annual PM2.5 concentration in Central China and the three provinces

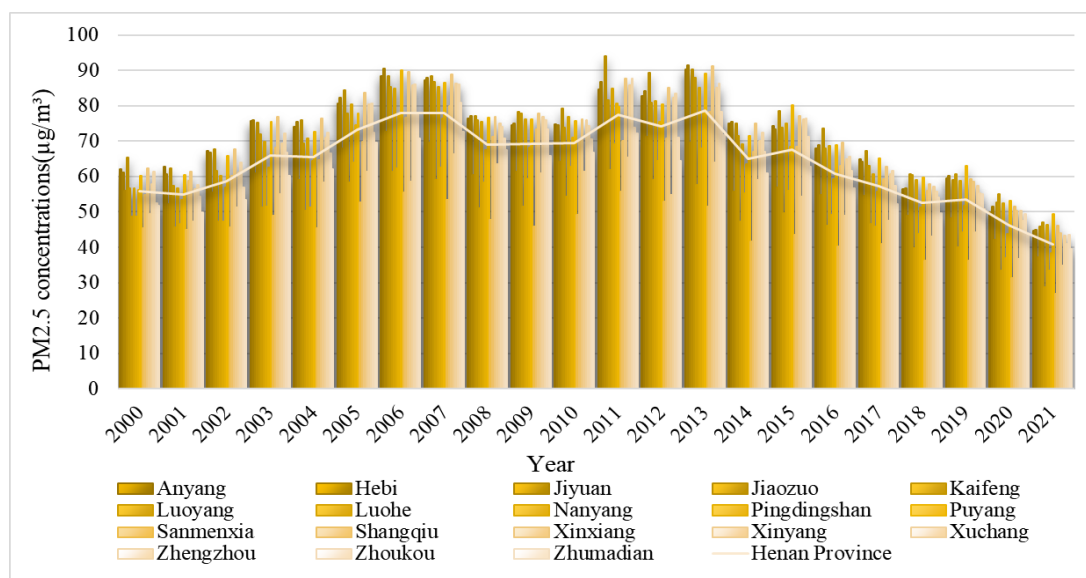


**Figure 3.** Variation trend of the average annual PM2.5 concentration of each city in Henan Province

From the perspective of each city in Hubei Province, as depicted in *Figure 4*, Tianmen and Xiantao exhibit the highest annual concentration of PM2.5 among the 17

cities examined. As industrialized cities, they house numerous factories and enterprises that emit substantial amounts of exhaust gases during production processes, including significant quantities of particulate matter - one of the primary sources of PM<sub>2.5</sub> pollution. Conversely, Enshi Prefecture, Shennongjia Forest District and Shiyan City display relatively low average annual concentrations due to their cleaner industrial structures with lower proportions of heavy industry and chemical manufacturing resulting in reduced emissions of pollutants. Notably, Shennongjia Forest area is China's only administrative division designated as a "forest area," boasting an impressive vegetation coverage rate at 96.7%. The abundant greenery has excellent adsorption capabilities for airborne particulate matter while also purifying it from the air - effectively reducing PM<sub>2.5</sub> levels.

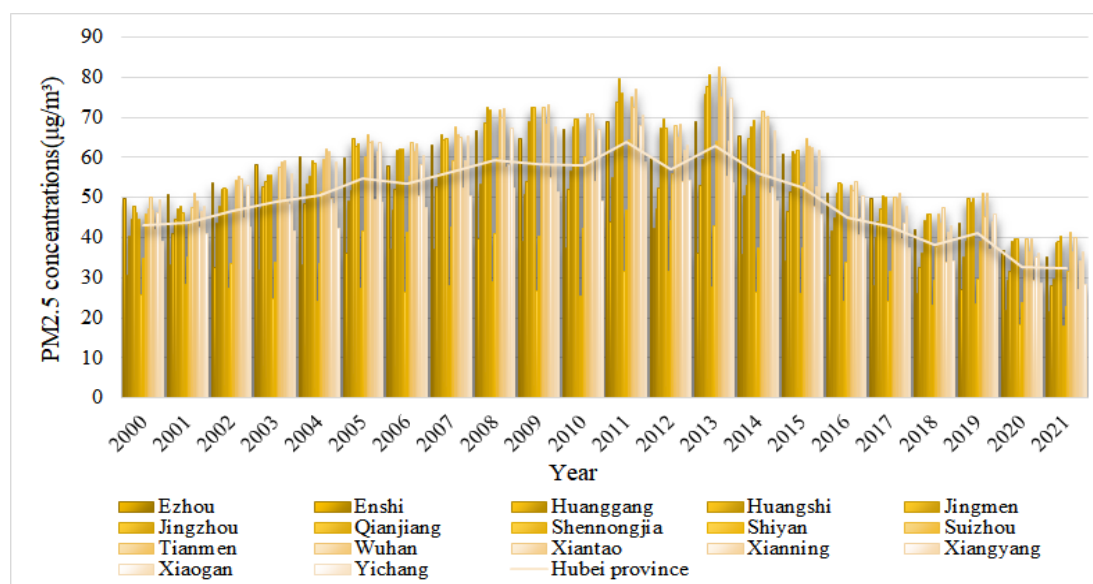


**Figure 4.** Variation trend of the average annual PM<sub>2.5</sub> concentration of each city in Hubei Province

From the perspective of each city in Hunan Province, as depicted in *Figure 5*, Xiangtan city exhibits the highest average annual PM<sub>2.5</sub> concentration among the 14 cities examined. The key pillar industries in Xiangtan city encompass mechanical and electrical engineering, metallurgy, textiles, chemicals, and building materials. These industries play a pivotal role in the economic development of Xiangtan City while significantly impacting PM<sub>2.5</sub> concentration through exhaust gas emissions and energy consumption. Conversely, Xiangxi Prefecture boasts a low average annual PM<sub>2.5</sub> concentration due to its abundant vegetation coverage and the presence of ecosystems such as forests and wetlands that contribute to air purification efforts.

In order to further analyze the temporal variation characteristics of PM<sub>2.5</sub> concentration in Central China, this study utilizes the annual average PM<sub>2.5</sub> concentration limit specified in the Ambient Air Quality Standard (GB3095-2012). The annual PM<sub>2.5</sub> concentration value is divided into four intervals, and an analysis is conducted on the proportion of districts and counties falling within each interval during the study period, as depicted in *Figure 6*. The findings indicate that, prior to 2018, there was a limited number of districts and counties in central China with an average annual

PM2.5 concentration below 35  $\mu\text{g}/\text{m}^3$ . Although the count of districts and counties exhibiting an average PM2.5 concentration below 35  $\mu\text{g}/\text{m}^3$  increased after 2018, a significant proportion still exceeded this threshold.

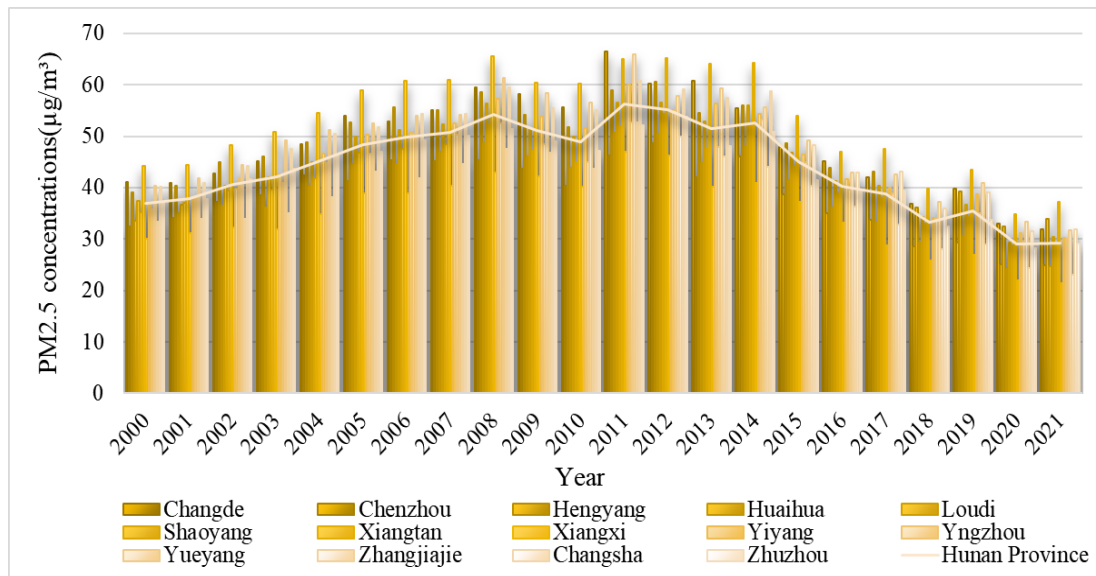


**Figure 5.** Variation trend of the average annual PM2.5 concentration of each city in Hunan Province

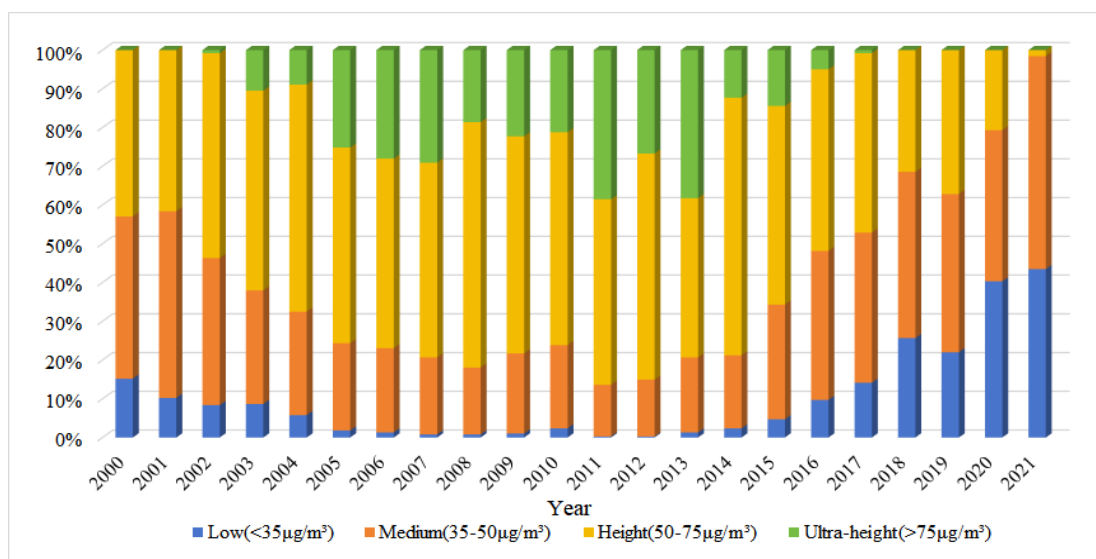


**Figure 6.** Trends of PM2.5 concentration changes by range in Central China in 2000–2021

### Spatial variation trend analysis of PM2.5 concentration

In order to analyze the spatial variation characteristics of PM2.5 concentration in Central China more intuitively, image data were extracted from the original PM2.5 remote sensing data for the years 2000, 2005, 2010, 2015, and 2020. The statistical analysis of PM2.5 concentration was conducted at a sub-division level based on county

administrative districts. The visualization results are presented in *Figure 7*. In all five selected years, Henan Province, particularly its northern region, consistently exhibited high levels of PM<sub>2.5</sub> pollution. It is evident that between 2000 and 2010, there was a gradual increase in average annual PM<sub>2.5</sub> concentration above 70  $\mu\text{g}/\text{m}^3$  across various districts and counties, indicating a north-to-south spreading trend within Henan Province. From 2015 to 2020, there has been a significant decrease in the number of districts and counties with an average annual PM<sub>2.5</sub> concentration above 70  $\mu\text{g}/\text{m}^3$ ; this suggests that central China's air quality has shown considerable improvement over the past five years. However, it should be noted that a large number of counties still experience an mean yearly PM<sub>2.5</sub> concentration above 35  $\mu\text{g}/\text{m}^3$ .

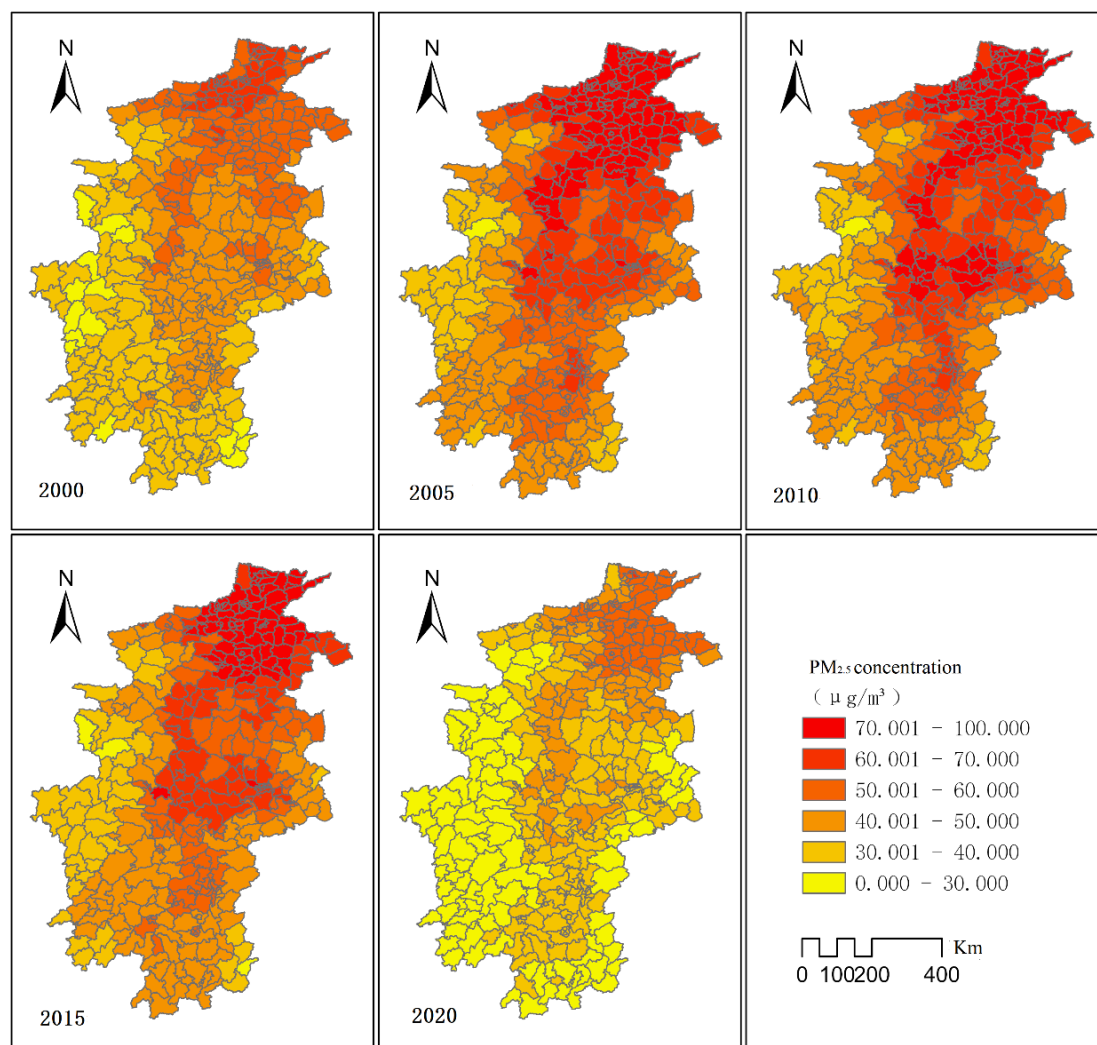


**Figure 7.** Spatial distribution of average annual PM<sub>2.5</sub> concentration in Central China

The SDE is employed in this study to quantitatively elucidate the centrality, directionality, and extensibility of the annual average PM<sub>2.5</sub> concentration in Central China from a global and spatiotemporal perspective. Only the findings for 2000, 2005, 2010, 2015, and 2020 are presented herein as delineated in *Table 3* and *Figure 8*.



**Table 3.** Standard deviation ellipse model parameters

Year	2000	2005	2010	2015	2020
Displacement of center of gravity/ km	–	1.395	13.393	12.120	8.714
Azimuth/°	12.362	12.560	12.571	12.840	12.754
Ellipse area/ km <sup>2</sup>	361224.589	345610.596	354757.107	354502.777	353032.094
Long axis standard deviation/ km	560.110	561.794	556.255	562.720	564.417
Short axis standard deviation/ km	205.294	200.931	203.016	200.539	199.107

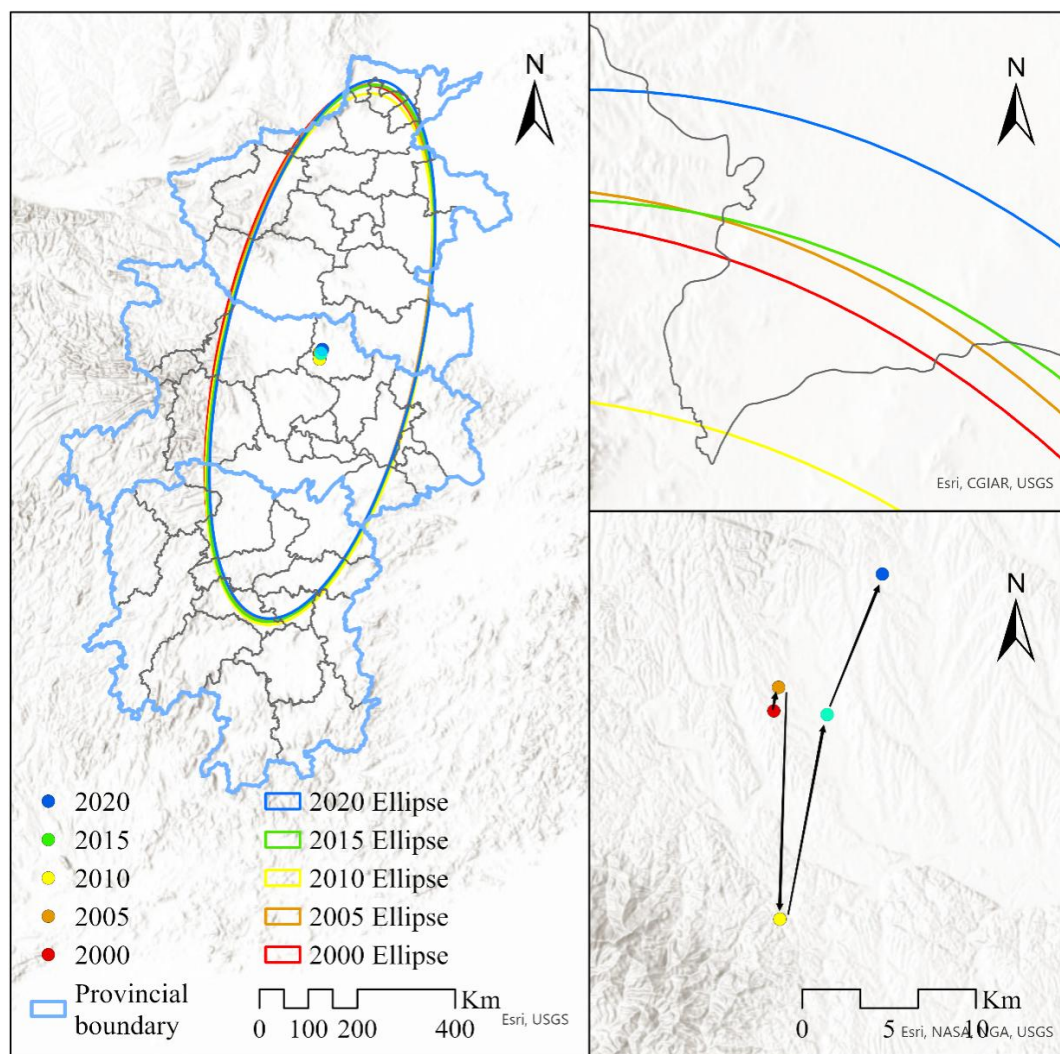


**Figure 8.** Spatial variation of the center of gravity and standard deviation ellipse of PM<sub>2.5</sub> concentration

From the perspective of spatial barycenter shift, the average annual PM<sub>2.5</sub> concentration in central China exhibited a slight northward shift of 1.395 km from 2000 to 2005, while the concentration center remained relatively stable. Subsequently, between 2005 and 2010, there was a significant southward movement of the PM<sub>2.5</sub> concentration center by approximately 13.393 km. Moreover, during the periods

spanning from 2010 to 2015 and from 2015 to 2020, there were successive northeastward shifts of approximately 12.840 km and 12.754 km respectively for the PM<sub>2.5</sub> concentration center within Central China region over these ten years; this trend is consistent with the spatial distribution pattern characterized by a “northeast-to-southwest” direction for PM<sub>2.5</sub> concentration within Central China region overall. On an overall basis, it can be inferred that there has been a gradual northward shift observed for the spatial barycenter of PM<sub>2.5</sub> concentration within Central China region over time.

From the perspective of azimuthal variation, the spatial distribution pattern of PM<sub>2.5</sub> concentration in Central China generally exhibits a “northeast-southwest” directionality, which is closely associated with the region’s geographical landform and population distribution. The fluctuation in rotation angle has increased from 12.362° in 2000 to 12.754° in 2020, indicating a weak tendency towards an “east-west” trend in the spatial distribution pattern of PM<sub>2.5</sub> pollution in Central China.

From the perspective of ellipse coverage, the area of the standard deviation ellipse exhibited an overall decreasing trend, declining from 361224.589 km<sup>2</sup> in 2000 to 345610.596 km<sup>2</sup> in 2005. However, between 2005 and 2010, it expanded to reach a maximum of 354757.107 km<sup>2</sup> before gradually contracting to 353032.094 km<sup>2</sup> in 2020. This indicates a pattern of “contraction-expansion-contraction” in its distribution range. Furthermore, the standard deviation ellipse for the five-year period primarily encompasses the northern and central regions of Henan and Hubei provinces, which are crucial areas for air pollution prevention and control efforts in Central China.

The difference between the length of the major and minor axes of the SDE exhibits a gradually increasing trend overall, thereby confirming the directional nature of PM<sub>2.5</sub> concentration spatial distribution. From the perspective of the major axis, there was an initial increase in its standard deviation from 560.110 km in 2000 to 561.794 km in 2005, indicating an expanding trend in average annual PM<sub>2.5</sub> concentration across Central China along the “northeast-to-southwest” direction, where highly polluted areas were concentrated. Subsequently, from 2005 to 2010, there was a decrease in the standard deviation of the major axis from 561.794 km to 556.255 km, suggesting a contraction trend in air pollution along this main direction during that period. Similarly, it can be observed that air pollution in Central China exhibited an alternating pattern of expansion and contraction along its main direction between 2000 and 2021, which aligns with changes seen in average annual PM<sub>2.5</sub> concentration over the past twenty-two years within this region as well. Furthermore, there is a general decreasing trend observed for the standard deviation of the minor axis, indicating an increased spatial centripetal force exerted by PM<sub>2.5</sub> concentration across central China.

### ***Spatial aggregation analysis of PM<sub>2.5</sub> concentration***

#### ***Global spatial autocorrelation analysis***

To achieve a thorough understanding of the spatial distribution characteristics of PM<sub>2.5</sub> in Central China, we analyzed the annual average PM<sub>2.5</sub> concentration data for the years 2000, 2005, 2010, 2015, and 2020. Using spatial autocorrelation analysis, we calculated the Moran index (Fig. 9) for these years. The results show that the Moran index is positive for all five years and passes the significance test at the 0.01 level. This indicates a significant positive spatial correlation and aggregation in PM<sub>2.5</sub> distribution across Central China. The strong spatial autocorrelation underscores the importance of

considering spatial heterogeneity when developing models to understand the driving mechanisms behind PM<sub>2.5</sub> concentrations.

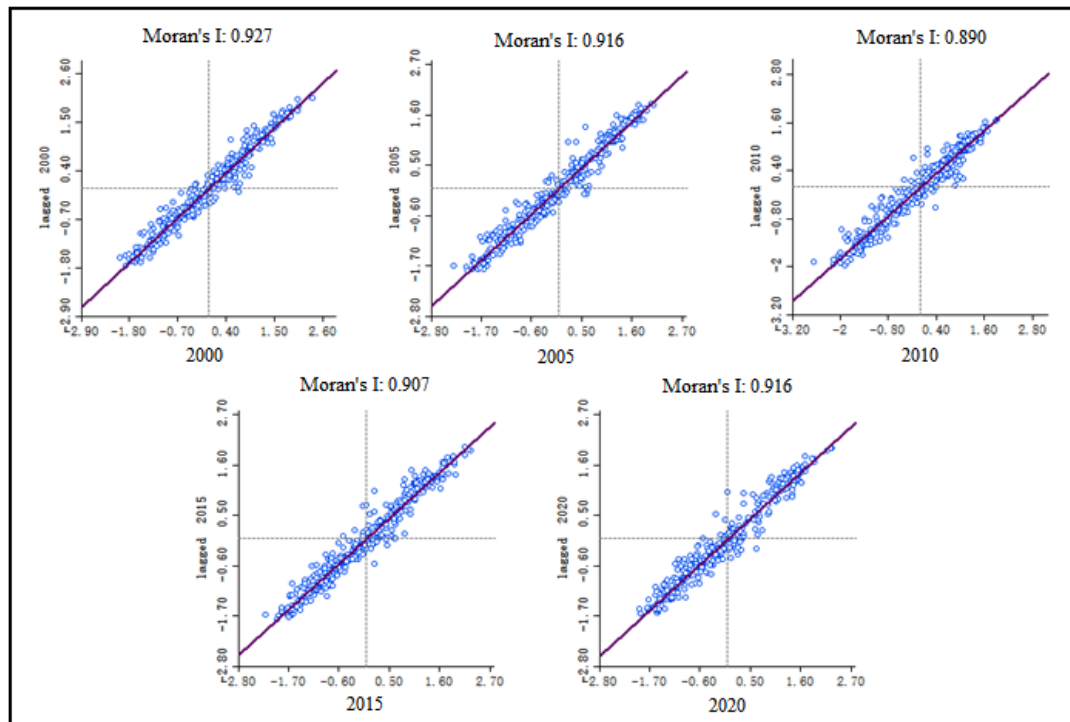


**Figure 9.** Moran's *I* index of PM<sub>2.5</sub> in 2000, 2005, 2010, 2015 and 2020

#### *Local spatial autocorrelation analysis*

To gain a deeper understanding of the spatial concentration characteristics of PM<sub>2.5</sub> in central China, we conducted a spatial Getis-Ord hot spot analysis on the satellite inversion data of PM<sub>2.5</sub>, building upon the findings from global spatial autocorrelation analysis. This analysis aimed to explore the spatial distribution patterns of local PM<sub>2.5</sub> concentrations. The results (Fig. 10) indicate that the study area as a whole exhibits strong aggregation during the period from 2000 to 2021, with certain areas in 2000, 2005, 2010, 2015 and 2020 showing significant aggregation at a confidence level of 99%. From a spatial perspective, high-spatially correlated hot spots are concentrated in central Henan Province and central Hubei Province; whereas low-spatially correlated cold spots are concentrated in Hunan Province and western Hubei Province. The distribution pattern of cold and hot spots for PM<sub>2.5</sub> concentrations remains relatively stable across central China; however, there have been some changes observed in terms of their size and number within different grades over time. Temporally speaking, there is an overall strengthening trend observed in the spatial autocorrelation of PM<sub>2.5</sub> in central China; notably, local autocorrelation is significantly stronger in 2020 compared to that in 2000. Spatially speaking, there is evidence suggesting southward diffusion trends for hot spots as they gradually spread from Henan province and central Hubei Province towards central Hunan Province.

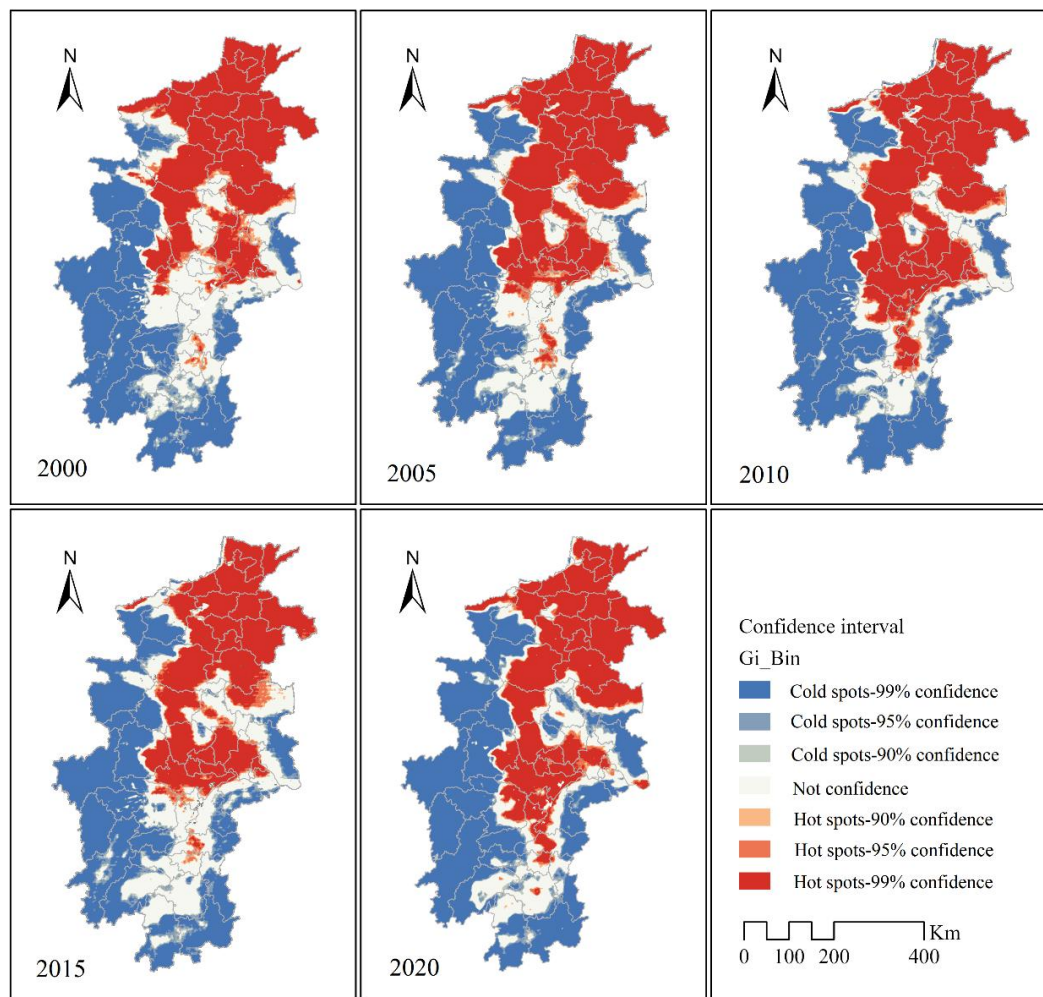


**Figure 10.** Distribution of PM2.5 spatial cold hot spots in 2000, 2005, 2010, 2015 and 2020

### *Analysis of the driving mechanism*

#### *Comparison of the GWR Model and MGWR model*

The present study utilizes 2020 PM2.5 and driver data to construct the driving mechanism of PM2.5. In order to obtain a driving model with improved fitting effect and closer approximation to real-world conditions, GWR and MGWR models were separately established at two levels of data units: grid sampling and county-level administrative division, with selection of models exhibiting superior goodness-of-fit for subsequent driving analysis.

Among them, raster sampling obtained 2948 basic data units of natural factors and socio-economic factors after random sampling in Central China and eliminating invalid sampling data. Subsequently, 383 basic data units of natural factors and socio-economic factors were obtained by averaging the influencing factors in each district and county through county-level administrative divisions. In the results of regression analysis, a higher goodness of fit  $R^2$  value indicates a better fitting effect and higher precision of the model. The AICC value also plays a role in determining the quality of fit, with smaller values indicating better performance. *Table 4* demonstrates that both datasets show higher goodness of fit  $R^2$  values in the MGWR model compared to the GWR.



**Table 4.** Comparison of GWR and MGWR models

Evaluation index	Raster sampling data		County-level data	
	GWR	MGWR	GWR	MGWR
R <sup>2</sup>	0.903	0.997	0.851	0.981
AICc	1510.133	-7337.479	374.799	-210.331

Additionally, the AICc value for the MGWR is significantly lower than that for the GWR. These findings suggest that the MGWR outperforms traditional GWR. Therefore, based on our data analysis results, it can be concluded that using an MGWR model yields greater accuracy when studying temporal and spatial characteristics as well as driving factors related to PM2.5 levels. Furthermore, it should be noted that raster sampling data exhibits superior goodness-of-fit measures (R<sup>2</sup>) and AICc values compared to district- or county-level data; thus, emphasizing how accurate spatial data impacts modeling outcomes when constructing PM2.5 driving models.

In *Figures 11* and *12*, R<sup>2</sup> represents the actual explanatory power of the natural and socio-economic indicators selected from the raster sampling data and district-level data on PM2.5 concentration impact levels. It is evident that both datasets' modeling results indicate a higher R<sup>2</sup> for MGWR compared to GWR. The results of MGWR models for both datasets reveal that over 80% of sample units have an R<sup>2</sup> greater than 0.85, further demonstrating the strong comprehensive interpretability of the selected impact factors on PM2.5 concentration in Central China.

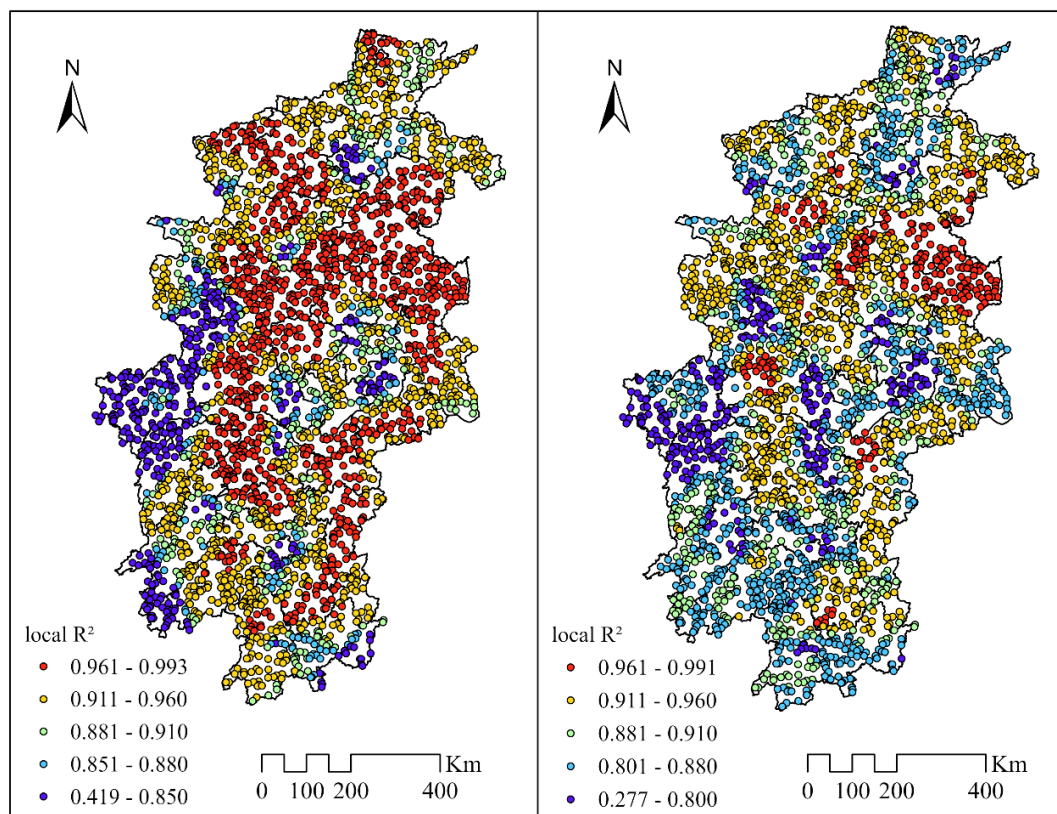


**Figure 11.** Comparison of local R<sup>2</sup> spatial distribution between GWR and MGWR fitting results from raster sampling

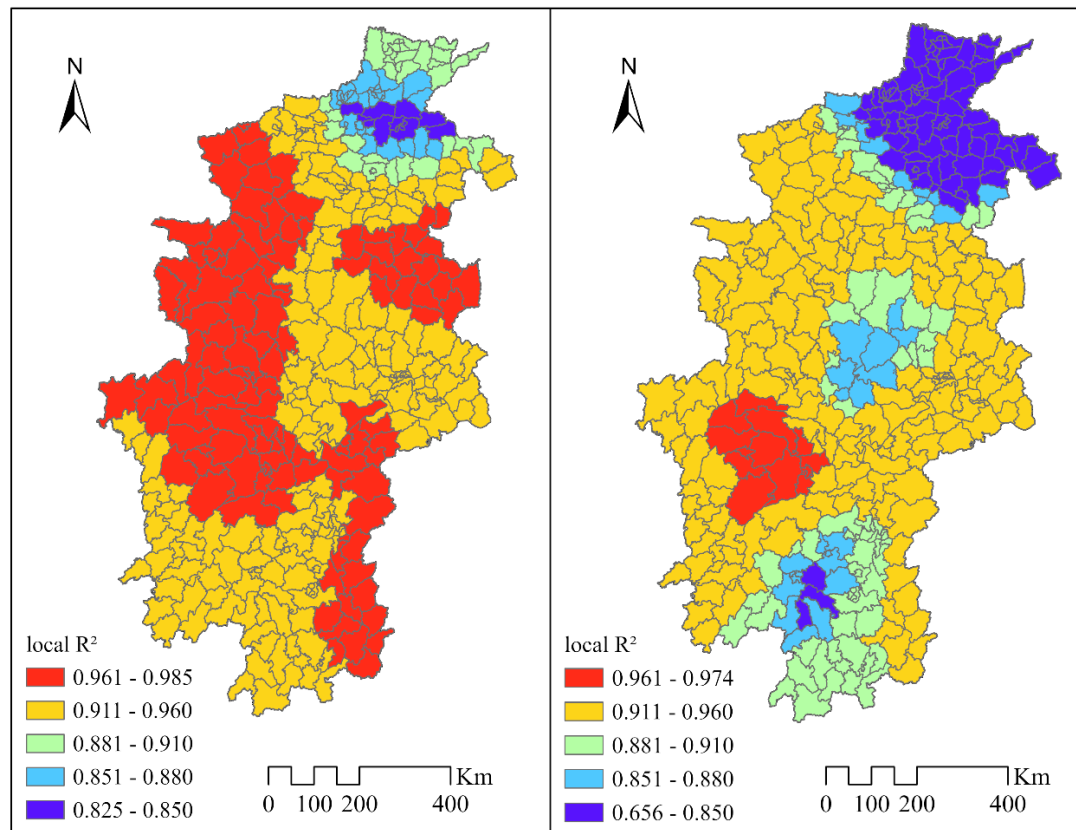


**Figure 12.** Comparison of local  $R^2$  spatial distribution between GWR and MGWR fitting results at district and county level

According to the bandwidth comparison between the GWR and MGWR (Table 5), it is apparent that the MGWR captures the varying influence scales of different variables, while the GWR only presents their average influence scales. The bandwidth of each variable quantifies the spatial influence scales of various driving factors, highlighting the disparities in the influence scales of different natural and socioeconomic factors on PM2.5. A larger influence scale signifies lower spatial heterogeneity in the factor's impact, whereas a smaller influence scale indicates greater spatial heterogeneity.

Among the natural factors, the impact magnitudes of air temperature, relative humidity, elevation, and precipitation are 46, 43, 44, and 43 respectively; all of which are relatively small (<78). Conversely, these factors have a significant influence on PM2.5 concentration levels. Additionally, there is spatial heterogeneity in the effect magnitudes of vegetation index (97) and average wind speed (140).

Among the socioeconomic factors, the impact magnitudes of night light and GDP on PM2.5 concentration are 44 and 43, respectively (<78), exhibiting significant spatial heterogeneity. Electricity consumption, population density, and proportion of arable land have impact magnitudes of 299, 349, and 555 on PM2.5 concentration, respectively; these factors also display certain levels of spatial heterogeneity. CO2 emission has an impact magnitude of 2947 on PM2.5 concentration, which is essentially equivalent to the total sample size; it represents a global variable with minimal spatial heterogeneity. The influence of CO2 emission on PM2.5 concentration remains consistent across central China.

**Table 5.** Bandwidth of GWR and MGWR results

Factor	Bandwidth of GWR	Bandwidth of MGWR
Intercept	78	43
X1: air temperature	78	46
X2: vegetation index	78	97
X3: wind speed	78	140
X4: relative humidity	78	43
X5: elevation	78	44
X6: precipitation	78	43
X7: nighttime light	78	44
X8: CO2 emission	78	2947
X9: electricity consumption	78	299
X10: population density	78	349
X11: GDP	78	43
X12: arable land area share	78	555

#### *Spatial pattern of regression coefficient coefficients of drivers*

The statistical depiction of each coefficient in the MGWR model is shown in Table 6. The MGWR model's estimated coefficients are indicated by the results utilizing standardized data and the proportion of each that influences coefficient of factor on PM2.5 concentrations' different directions. Spatial heterogeneousness is revealed by the regression coefficients that are obtained from the multi-scale geographical weighted regression (MGWR) model in each variable's effects on regional PM2.5 concentration. All CO2 emissions exhibit positive effects, while average wind speed, night light, and GDP predominantly demonstrate positive effects, accounting for 74.898%, 71.744%, and 85.583% of total samples, respectively. The impact of air temperature and electricity consumption on PM2.5 exhibited a polarizing effect, with an equal distribution of positive and negative effects. The vegetation index, relative humidity, elevation, precipitation, population density, and cultivated land area exerted inhibitory influences on PM2.5 levels, accounting for 82.598%, 85.753%, 74.152%, 95.522%, 73.202%, and 66.418% of the total sample, respectively.

**Table 6.** Parameter estimation for regression of PM2.5 concentration using MGWR

Variables	Mean	Min	Max	+	-
Intercept	0.156	-0.651	1.056	59.837	40.163
X1: air temperature	-0.003	-0.502	0.340	51.696	48.304
X2: vegetation index	-0.021	-0.108	0.074	17.402	82.598
X3: wind speed	0.016	-0.033	0.089	74.898	25.102
X4: relative humidity	-0.074	-0.332	0.221	14.247	85.753
X5: elevation	-0.087	-0.398	0.146	25.848	74.152
X6: precipitation	-0.428	-0.813	0.259	4.478	95.522
X7: nighttime light	0.022	-0.132	0.129	71.744	28.256
X8: CO2 emission	0.008	0.007	0.008	100.000	0.000
X9: electricity consumption	-0.004	-0.058	0.067	46.574	53.426
X10: population density	-0.006	-0.026	0.014	26.798	73.202
X11: GDP	0.186	-0.127	0.947	85.583	14.417
X12: arable land area share	-0.001	-0.010	0.010	33.582	66.418



The natural class factors are illustrated in *Figure 13*. (1) The influence of air temperature on PM<sub>2.5</sub> concentration exhibits significant spatial heterogeneity, with a promoting effect observed in most areas of northwest Henan Province and Hubei Province. However, the concentration of PM<sub>2.5</sub> is inhibited in most parts of Hunan Province. (2) The vegetation index predominantly inhibits PM<sub>2.5</sub> concentration across most areas. Nevertheless, there are exceptions where promotion effects on PM<sub>2.5</sub> concentration are observed in the northern part of Henan Province, central part of Hubei Province, and southwest part of Hunan Province. (3) Average wind speed primarily exerts a positive impact on PM<sub>2.5</sub> concentration in Central China; however, it shows an inhibitory effect only in the southeast region of Hunan Province and eastern part of Henan Province regarding PM<sub>2.5</sub> levels. This suggests that under specific wind speed conditions, particulate matter may be suspended and propagated by wind currents leading to increased concentrations of PM<sub>2.5</sub>.

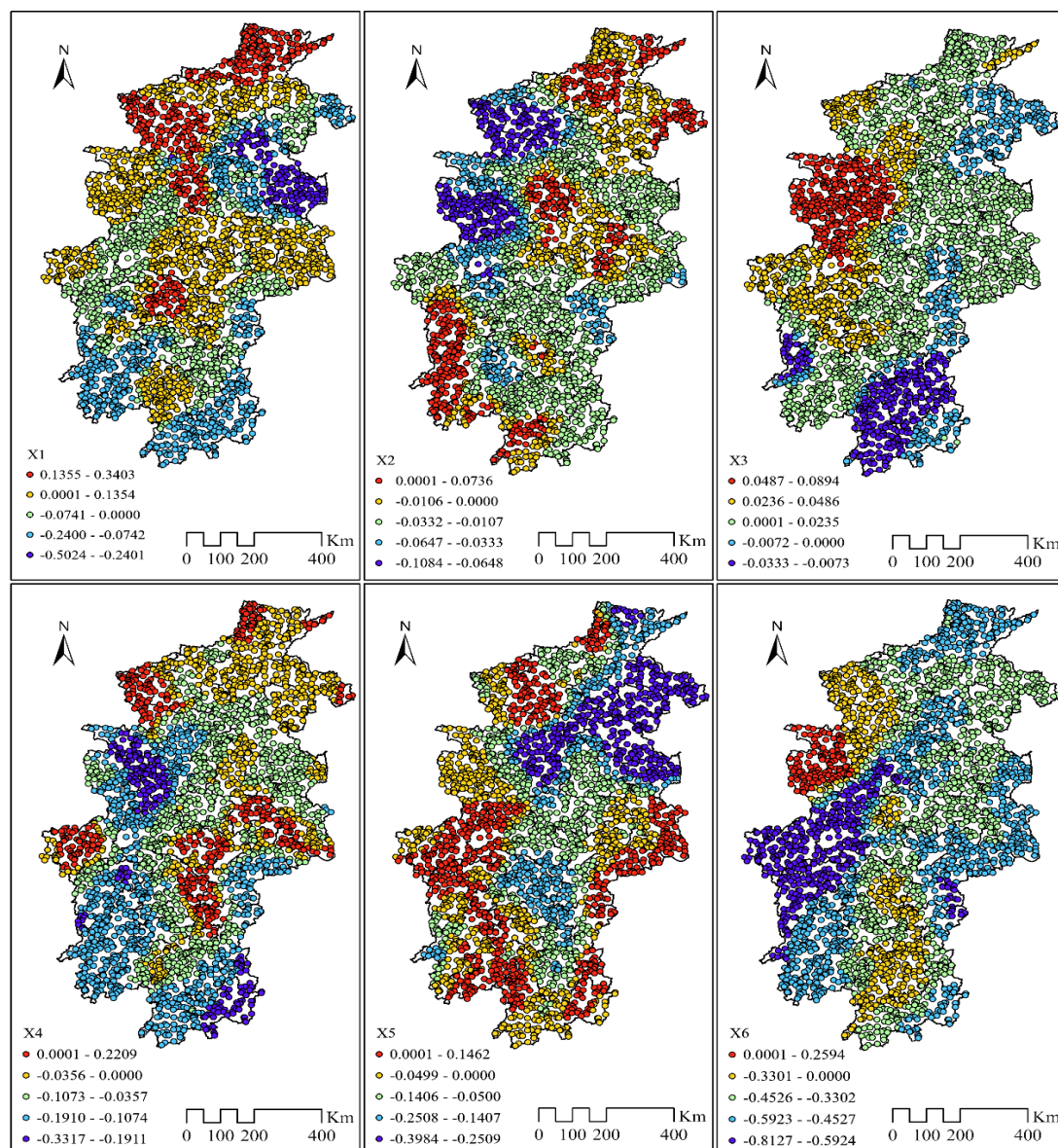


**Figure 13.** Spatial pattern of multi-scale geographical weighted regression coefficients -- natural class factors

(4) The influence of relative humidity on PM2.5 concentration in central China is mainly inhibition. Only in Henan, Hubei, the western mountainous areas of the two Lakes basin and other small areas showed a positive effect, and in the rest of the region showed an inhibitory effect on PM2.5 concentration. (5) Elevation significantly inhibits PM2.5 concentration in most areas of Central China but only shows a promotion effect in some mountainous regions. (6) Precipitation mainly suppresses PM2.5 levels except for Shiyan City's western region where it has a positive promoting effect on PM2.5 concentration possibly influenced by other environmental factors such as precipitation intensity. Overall, higher precipitation enhances the clearance rate of PM2.5 particles.

The socioeconomic factors are shown in *Figure 14*: (1) Night light has a positive impact on PM2.5 concentration in most regions of central China, particularly in certain mountainous areas such as Anyang City, Shiyan City, and Huaihua City. This phenomenon can be attributed to the influence of variations in mountain terrain height on the accuracy of night light inversion data. To some extent, night light data can serve as an indicator of human activities and socioeconomic parameters. In other words, the positive effect of night light on PM2.5 concentration is comparable to that of GDP on PM2.5 concentration. (2) CO2 emissions in Central China exert a observable positive effect on PM2.5 concentration, with this impact's intensity bit by bit increasing from north-east to south-west. (3) Electricity consumption in northeast Henan, western Hubei, western Hunan, and southern Hunan exhibited a positive correlation with PM2.5 concentration. In contrast, the rest of the region experienced a decrease in PM2.5 levels. (4) The population density in central China predominantly suppressed PM2.5 concentration but had an enhancing effect only in the eastern Henan Plain and Lianghu Basin areas. (5) GDP exerts a positive effect on PM2.5 concentration primarily in Central China. There, however, exists a disadvantageous correlation between PM2.5 concentration and GDP merely in certain areas of the eastern Henan Plain and the two Lake basins. (6) The proportion of cultivated land area exhibits significant spatial heterogeneity, leading to an elevation of PM2.5 concentration across most parts of Henan Province and the region bordering Huanggang City and Huangshi City; conversely, it inhibits PM2.5 concentration in other areas.

## Discussion

Through the analysis of the spatiotemporal evolution characteristics of PM2.5 concentration in provinces, cities, and counties in the central region, it is found that the central region is generally a more serious area of PM2.5 pollution. Specifically, Henan province has the highest PM2.5 concentration among the three provinces studied, highlighting the priority of air environment management in Henan Province. This finding is consistent with previous research by Ge et al. (2022). We observe that over a span of more than 20 years, the inflection point of the annual average concentration variation in three provinces located in Central China consistently coincides with the promulgation of environmental governance policy documents or legislation by relevant administrative authorities. For instance, in 2011, the Environmental Protection Department of Hubei Province issued the "Hubei Province 2011 Comprehensive Plan for Controlling Major Pollutant Emissions," while in 2013, The State Council released the "Guidance on Resolving Severe Overcapacity Contradictions." Additionally, Henan Province's Department of Ecological Environment enacted the "Henan Province Regulations on Air Pollution Prevention" and other pertinent policies. This

demonstrates that rational policies can be formulated and implemented to effectively mitigate PM2.5 pollution. It is worth noting that the results of spatial correlation analysis and the standard deviation ellipse model demonstrate a significant regional synergistic effect of PM2.5 pollution, with the potential to propagate to surrounding areas. Therefore, it is imperative to adopt a holistic approach towards atmospheric environmental governance in order to achieve an overall effect greater than the sum of its parts.

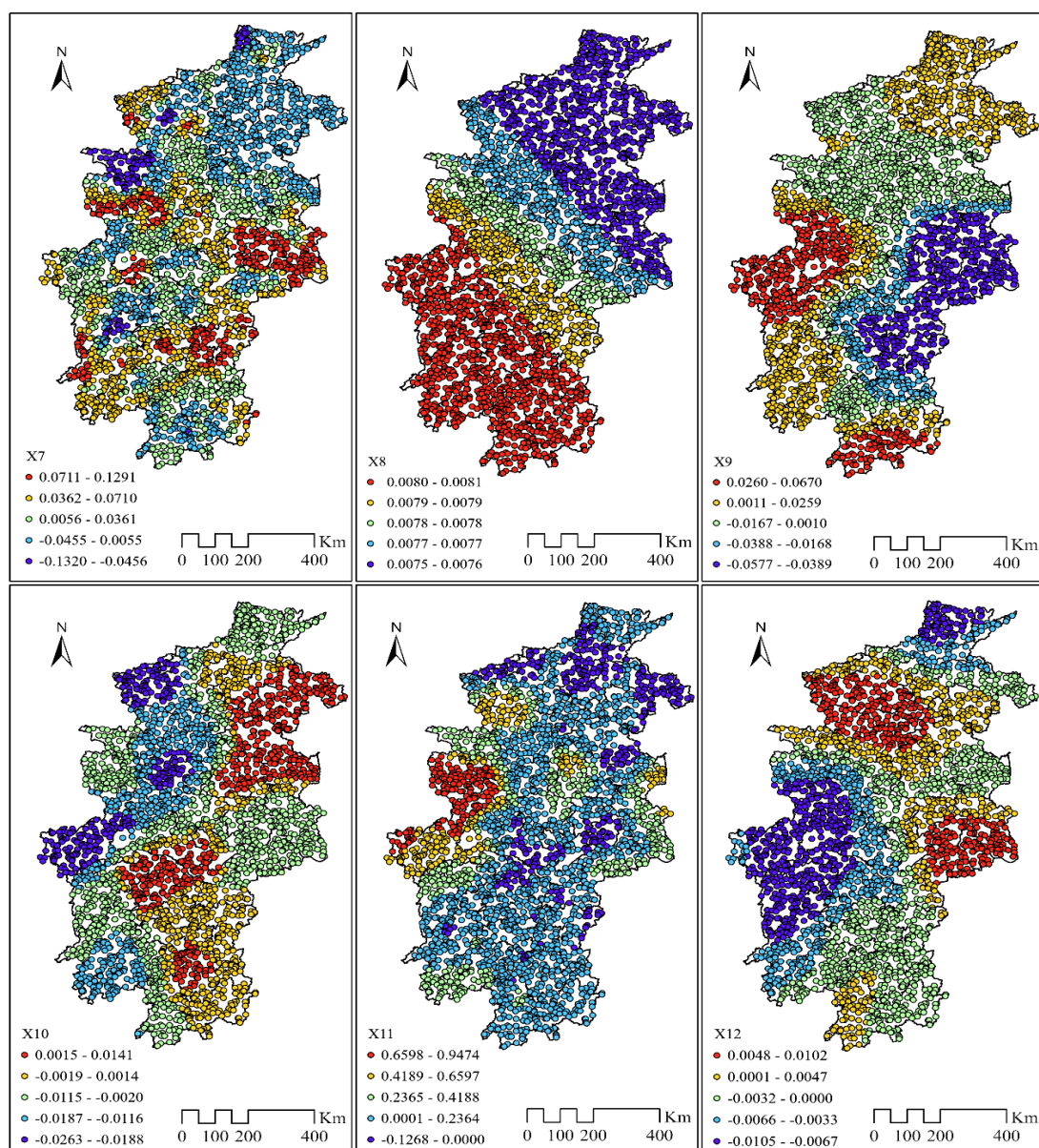


**Figure 14.** Spatial pattern of multi-scale geographical weighted regression coefficients -- socioeconomic factors

According to the drive model results, only the impact of CO2 emissions on PM2.5 in Central China exhibits a positive correlation with the overall situation. This pattern emerges owing to the main source of CO2 emissions being the combustion of fossil



fuels such as coal, petroleum, and natural gas throughout industrial output processes. This implies that policymakers should fully consider the CO<sub>2</sub> emission index, particularly emphasizing the significance of large emission sources such as large-scale industrial production, and actively promote energy conservation and emission reduction across daily life and production activities. The primary factors positively influencing PM<sub>2.5</sub> levels include wind speed, night light, and GDP. This contrasts with the findings of Wang et al. (2020), where wind speed had a negative effect. However, due to low average annual wind speeds in central China leading to poor air flow diffusion, pollutants react with each other during transmission, exacerbating PM<sub>2.5</sub> pollution. Night light and GDP objectively reflect regional development levels but also contribute to certain environmental pollution during social industrialization and modernization processes. Nevertheless, there are still instances where GDP and night light exhibit a restraining effect on PM<sub>2.5</sub> levels, indicating that development can be coordinated with environmental concerns. Therefore, all regions should proactively explore green industries suitable for their specific circumstances.

The spatial distribution of PM<sub>2.5</sub> concentration is influenced by air temperature and electricity consumption, exhibiting a distinct polarized pattern. In plain areas, higher air temperatures promote convective activities, facilitating the diffusion of pollutants and enabling convective rain to effectively remove PM<sub>2.5</sub>. Conversely, in mountainous and undulating regions, temperature inversion occurs more frequently, leading to local accumulation of atmospheric pollutants (Zhou et al., 2021) and exacerbating pollution levels. The primary factor contributing to the polarization of the impact of electricity consumption on PM<sub>2.5</sub> concentration lies in the divergence of electricity sources, with some regions relying on coal combustion for power generation while others utilize cleaner methods such as hydropower or wind power. This disparity in power generation modes inherently determines the varying effects of electricity consumption on PM<sub>2.5</sub> levels.

The vegetation index, relative humidity, altitude, precipitation, population density, and the proportion of cultivated land area exhibited inhibitory effects on PM<sub>2.5</sub> concentration in most regions. Among these factors, the impact of the vegetation index can be attributed to its role in adsorbing and retarding fine particles in the atmosphere. However, a positive effect was observed in a small portion of the land which may be attributed to variations in vegetation types. Therefore, increasing vegetation coverage has a certain degree of efficacy in mitigating PM<sub>2.5</sub> pollution. The negative impact of relative humidity on PM<sub>2.5</sub> is attributed to the precipitation resulting from relative humidity surpassing a specific threshold, which facilitates the settling of PM<sub>2.5</sub> particles. Conversely, in other regions, the positive effect arises from the occurrence of temperature inversions near ground level as relative humidity increases without exceeding the threshold. This condition hampers particulate matter diffusion but promotes hygroscopic growth and water-phase formation of secondary particulate matter, consequently elevating PM<sub>2.5</sub> concentration. The impact of elevation on PM<sub>2.5</sub> varies across spatial regions, indicating that altitude significantly influences the formation and transport of PM<sub>2.5</sub>. Therefore, the impact of elevation cannot be ignored when considering the role of other factors on PM<sub>2.5</sub>. Precipitation mainly inhibited PM<sub>2.5</sub>, accounting for 95.522% of the total sample size. This is because the precipitation process can wash the particles in the air, and it also has a certain inhibitory effect on the dust on the surface. The impact of population density on PM<sub>2.5</sub> primarily exhibits an inhibitory effect, accounting for 73.202% of the total sample size. Population density itself does not directly induce fluctuations in PM<sub>2.5</sub> levels; however,

it indirectly influences these levels through interactions with individuals' lifestyles and regional industrial and energy structures. This indicates that recent efforts to optimize new energy consumption patterns and industrial structure in central China have yielded certain achievements. There was significant spatial heterogeneity observed in the impact of cultivated land proportion on PM2.5 concentrations. This can be attributed to the varying effects of different types of cultivated land on PM2.5 levels, as well as the differential adsorption capacities exhibited by dry land and paddy fields towards PM2.5 particles. For instance, in Henan Province, where dry land dominates the agricultural landscape, activities such as straw burning directly contribute to substantial emissions of PM2.5 particles into the atmosphere. Conversely, paddy fields mitigate surface exposure and dust pollution through vegetation cover and evaporation processes, indirectly leading to a reduction in PM2.5 concentrations.

By comparing the results of raster sampling data modeling and county-level administrative division data modeling, we not only find that MGWR outperforms the GWR model in analyzing the relationship between multiple spatial attribute data but also draws our attention to the impact of varying data accuracy on spatial modeling analysis. This provides us with a clear direction for further research, namely, to employ higher spatially accurate data for modeling analysis.

## Conclusion

The influence of PM2.5 on air quality and public health has garnered increasing attention, making a pivotal research topic for it in the fields of environmental science and public health. This research concentrates on central China as the study topic, meticulously looking through the spatiotemporal distribution characteristics of PM2.5 in this area through using remote sensing data from 2000 to 2021. Through comprehensive analysis spanning 22 years, the temporal evolution trend and spatial distribution pattern of PM2.5 pollution is unveiled by us whereas building a driving model to elucidate the impacts exerted by using natural and socioeconomic factors on PM2.5 concentration. The aforementioned analysis leads to the following conclusions:

(1) In the past 22 years, the PM2.5 concentration in three provinces in Central China exhibited an initial upward trend followed by a subsequent decline, reaching its peak around 2012. Among these provinces, Henan province recorded the highest average annual PM2.5 concentration, while Hubei and Hunan experienced a similar situation with Hubei having a higher average annual PM2.5 concentration compared to Hunan province. Although some progress has been made in recent years regarding PM2.5 control, the average annual PM2.5 concentration in most districts and counties in Central China still exceeds the national Class II standard, indicating that there is still much work to be done towards mitigating PM2.5 pollution in this region.

(2) The concentration of PM2.5 in central China during the period from 2000 to 2021 exhibits evident spatial autocorrelation and significant spatial aggregation, implying that the regional interdependence effect of PM2.5 needs to be considered when analyzing its spatio-temporal variation characteristics. Overall, the centroid of PM2.5 concentration in central China demonstrates a tendency towards northeastward movement. Henan Province and northern Hubei Province are pivotal areas for air pollution prevention and control efforts in central China.

(3) Using the MGWR model to construct the PM2.5 driving mechanism allows for the identification of influencing factors at different spatial scales, providing a more



accurate fit compared to the GWR model. Both models' results suggest that the MGWR model is more effective for examining the factors driving PM<sub>2.5</sub> concentrations in Central China. Moreover, results obtained from raster data sampling and district-level data modeling demonstrate that the accuracy of spatial data has a certain impact on the quality of modeling outcomes. The future research work should therefore focus on high-precision spatial data modeling and acquisition, aiming to obtain analysis results that closely align with the actual situation.

(4) The MGWR model's regression coefficients demonstrate the varying levels of spatial heterogeneity in how each factor affects PM<sub>2.5</sub> concentrations in Central China. It is crucial to consider this spatial heterogeneity when modeling and analyzing data with spatial attributes. Simultaneously, this also demonstrates the necessity of fully integrating local circumstances when formulating environmental protection policies related to PM<sub>2.5</sub> suppression and thoroughly investigating the extent and direction of different driving factors' impact on PM<sub>2.5</sub> in order to develop scientifically sound and efficient environmental protection policies.

**Funding.** This work was supported in part by the Key scientific and technological projects in Henan Province under Grant 242102210017; the Key Scientific Research Projects of Colleges in Henan Province under Grant 23A520001.

## REFERENCES

- [1] Chang, J. H., Tseng, C. Y. (2017): Analysis of correlation between secondary PM<sub>2.5</sub> and factory pollution sources by using ANN and the correlation coefficient. – *IEEE Access* 5: 22812-22822.
- [2] Chen, L., Zhang, X., He, F., Yuan, R. (2019): Regional green development level and its spatial relationship under the constraints of haze in China. – *Journal of Cleaner Production* 210: 376-387.
- [3] Chen, Z., Chen, D., Zhao, C., Kwan, M.-P., Cai, J., Zhuang, Y., Zhao, B., Wang, X. (2020): Influence of meteorological conditions on PM<sub>2.5</sub> concentrations across China: a review of methodology and mechanism. – *Environment International* 139: 105558.
- [4] Fan, P., Xu, L., Yue, W., Chen, J. (2017): Accessibility of public urban green space in an urban periphery: the case of Shanghai. – *Landscape and Urban Planning* 165: 177-192.
- [5] Fang, C., Wang, Z., Xu, G. (2016): Spatial-temporal characteristics of PM<sub>2.5</sub> in China: a city-level perspective analysis. – *Journal of Geographical Sciences* 26: 1519-1532.
- [6] Fang, K., Wang, T. T., He, J. J., Shen, Y. (2020): Spatiotemporal variation and driving factors of NO<sub>2</sub> concentrations in the Belt and Road region. – *Acta Ecologica Sinica* 40(13): 4241-4251.
- [7] Fotheringham, A. S., Yang, W., Kang, W. (2017): Multiscale geographically weighted regression (MGWR). – *Annals of the American Association of Geographers* 107: 1247-1265.
- [8] Ge, Q. X., Liu, Y., Yang, H., Guo, H. L. (2022): Analysis on spatial-temporal characteristics and driving factors of PM<sub>2.5</sub> Henan Province from 2015 to 2019. – *Environmental Science* 43(04): 1697-1705.
- [9] Gu, J., Bai, Z., Liu, A., Wu, L., Xie, Y., Li, W., Dong, H., Zhang, X. (2010): Characterization of atmospheric organic carbon and element carbon of PM<sub>2.5</sub> and PM<sub>10</sub> at Tianjin, China. – *Aerosol and Air Quality Research* 10: 167-176.
- [10] He, C., Hong, S., Mu, H., Tu, P., Yang, L., Ke, B., Huang, J. (2021): Characteristics and meteorological factors of severe haze pollution in China. – *Advances in Meteorology* 2021: 6680564.

- [11] He, L., Lin, A., Chen, X., Zhou, H., Zhou, Z., He, P. (2019): Assessment of MERRA-2 surface PM2.5 over the Yangtze River Basin: ground-based verification, spatiotemporal distribution and meteorological dependence. – *Remote Sensing* 11(4): 460.
- [12] Huang, C., Liu, K., Zhou, L. (2021): Spatio-temporal trends and influencing factors of PM2.5 concentrations in urban agglomerations in China between 2000 and 2016. – *Environmental Science and Pollution Research* 28: 10988-11000.
- [13] Huang, Y. Y., Zhu, S. J., Wang, S. J. (2020): Driving force behind PM2.5 pollution in Guangdong Province based on the interaction effect of institutional background and socioeconomic activities. – *Tropical Geography* 40(01): 74-87.
- [14] Jiang, W., Gao, W., Gao, X., Ma, M., Zhou, M., Du, K., Ma, X. (2021): Spatio-temporal heterogeneity of air pollution and its key influencing factors in the Yellow River Economic Belt of China from 2014 to 2019. – *Journal of Environmental Management* 296: 113172.
- [15] Lin, G., Fu, J., Jiang, D., Hu, W., Dong, D., Huang, Y., Zhao, M. (2014): Spatio-temporal variation of PM2.5 concentrations and their relationship with geographic and socioeconomic factors in China. – *International Journal of Environmental Research and Public Health* 11(1): 173-186.
- [16] Liu, X., Zou, B., Feng, H., Liu, N., Zhang, H. (2020): Anthropogenic factors of PM2.5 distributions in China's major urban agglomerations: a spatial-temporal analysis. – *Journal of Cleaner Production* 264: 121709.
- [17] Luo, J., Du, P., Samat, A., Xia, J., Che, M., Xue, Z. (2017): Spatiotemporal pattern of PM2.5 concentrations in mainland China and analysis of its influencing factors using geographically weighted regression. – *Scientific Reports* 7: 40607.
- [18] Ouyang, W., Gao, B., Cheng, H., Hao, Z., Wu, N. (2018): Exposure inequality assessment for PM2.5 and the potential association with environmental health in Beijing. – *Science of The Total Environment* 635: 769-778.
- [19] Shen, Y., Zhang, L., Fang, X., Ji, H., Li, X., Zhao, Z. (2019): Spatiotemporal patterns of recent PM2.5 concentrations over typical urban agglomerations in China. – *Science of the Total Environment* 655: 13-26.
- [20] Shi, Y., Matsunaga, T., Yamaguchi, Y., Li, Z., Gu, X., Chen, X. (2018): Long-term trends and spatial patterns of satellite-retrieved PM2.5 concentrations in South and Southeast Asia from 1999 to 2014. – *Science of the Total Environment* 615: 177-186.
- [21] Tu, Y., Jiang, L. L., Liu, R., Xiao, Z. L., Min, J. (2021): Spatiotemporal changes of vegetation NDVI and its driving forces in China during 1982-2015. – *J Agric Eng-Italy* 37(22)75-84.
- [22] Wang, H., Chen, Z., Zhang, P. (2022): Spatial autocorrelation and temporal convergence of PM2.5 concentrations in Chinese cities. – *International Journal of Environmental Research and Public Health* 19(21): 13942.
- [23] Wang, S. J., Gao, S., Chen, J. (2020): Spatial heterogeneity of driving factors of urban haze pollution in China based on GWR model. – *Geographical Research* 39(03): 651-668.
- [24] Wang, Y., Wang, F., Min, R., Song, G., Song, H., Zhai, S., Xia, H., Zhang, H., Ru, X. (2023): Contribution of local and surrounding anthropogenic emissions to a particulate matter pollution episode in Zhengzhou, Henan, China. – *Scientific Reports* 13: 8771.
- [25] Xie, Y., Dai, H., Dong, H., Hanaoka, T., Masui, T. (2016): Economic impacts from PM2.5 pollution-related health effects in China: a provincial-level analysis. – *Environmental Science & Technology* 50: 4836-4843.
- [26] Yan, D., Zhou, M., Diao, Y., Yang, M. (2022): Air pollution in China: Spatial patterns and spatial coupling with population and economy. – *Front. Environ. Sci.* 10. <https://doi.org/10.3389/fenvs.2022.1040131>.
- [27] Yang, L., Hong, S., He, C., Huang, J., Ye, Z., Cai, B., Yu, S., Wang, Y., WANG, Z. (2022a): Spatio-temporal heterogeneity of the relationships between pm2.5 and its determinants: a case study of Chinese cities in winter of 2020. – *Front. Public Health* 10. <https://doi.org/10.3389/fpubh.2022.810098>.

- [28] Yang, T., Zhou, K., Ding, T. (2022b): Air pollution impacts on public health: evidence from 110 cities in Yangtze River Economic Belt of China. – *Science of the Total Environment* 851: 158125.
- [29] Yu, H., Fotheringham, A. S., Li, Z., Oshan, T., Kang, W., Wolf, L. J. (2020): Inference in multiscale geographically weighted regression. – *Geographical Analysis* 52: 87-106.
- [30] Yuan, W., Sun, H., Chen, Y., Xia, X. (2021): Spatio-temporal evolution and spatial heterogeneity of influencing factors of SO2 emissions in Chinese cities: fresh evidence from MGWR. – *Sustainability* 13.
- [31] Zhang, T., Liu, P., Sun, X., Zhang, C., Wang, M., Xu, J., Pu, S., Huang, L. (2020): Application of an advanced spatiotemporal model for PM2.5 prediction in Jiangsu Province, China. – *Chemosphere* 246: 125563.
- [32] Zhao, H., Liu, Y., Gu, T., Zheng, H., Wang, Z., Yang, D. (2022): Identifying spatiotemporal heterogeneity of PM2.5 concentrations and the key influencing factors in the middle and lower reaches of the Yellow River. – *Remote Sensing* 14(11): 2643.
- [33] Zhou, Z. L., Cheng, X. F. (2021): Spatial heterogeneity of influencing factors of PM2.5 in Chinese cities based on MGWR model. – *China Environmental Science* 41(6): 2552-2561.
- [34] Zhu, M., Guo, J., Zhou, Y., Cheng, X. (2022): Exploring the spatiotemporal evolution and socioeconomic determinants of PM2.5 distribution and its hierarchical management policies in 366 Chinese cities. – *Front. Public Health* 10. <https://doi.org/10.3389/fpubh.2022.843862>.